

AD-A024109

RIA-76-U199

Cy No. 1

# TECHNICAL LIBRARY

AD

A024109

R-TR-75042

USADACS Technical Library



5 0712 01001339 8

## THE SPUTTER DEPOSITION AND EVALUATION OF TUNGSTEN AND CHROMIUM COATINGS FOR USE IN WEAPON COMPONENTS

R.H. JONES, R.W. MOSS,  
E.D. McCLANAHAN & H.L. BUTTS

OCTOBER 1975

### TECHNICAL REPORT



PREPARED BY **PACIFIC NORTHWEST LABORATORIES**  
a division of  
**Battelle Memorial Institute**  
P.O. Box 999  
**Richland, Washington 99352**

#### DISTRIBUTION STATEMENT

Approved for public release, distribution unlimited.

PREPARED FOR

RESEARCH DIRECTORATE  
**GENERAL THOMAS J. RODMAN LABORATORY**  
**ROCK ISLAND ARSENAL**  
**ROCK ISLAND, ILLINOIS 61201**

**DISPOSITION INSTRUCTIONS:**

Destroy this report when it is no longer needed. Do not return it to the originator.

**DISCLAIMER:**

The findings of this report are not to be construed as an official Department of the Army position unless so designated by other authorized documents.

The citation of commercial products in this report does not constitute an official indorsement or approval of such products.

UNCLASSIFIED

SECURITY CLASSIFICATION OF THIS PAGE (When Data Entered)

REPORT DOCUMENTATION PAGE		READ INSTRUCTIONS BEFORE COMPLETING FORM
1. REPORT NUMBER R-TR-75042	2. GOVT ACCESSION NO.	3. RECIPIENT'S CATALOG NUMBER
4. TITLE (and Subtitle) THE SPUTTER DEPOSITION AND EVALUATION OF TUNGSTEN AND CHROMIUM FOR USE IN WEAPON COMPONENTS		5. TYPE OF REPORT & PERIOD COVERED Technical Report
		6. PERFORMING ORG. REPORT NUMBER
7. AUTHOR(s) R.H. Jones, R.W. Moss, E.D. McClanahan and H.L. Butts		8. CONTRACT OR GRANT NUMBER(s) MIPR M5-4-P0048-01-M5-W3
9. PERFORMING ORGANIZATION NAME AND ADDRESS Pacific Northwest Laboratories a division of Battelle Memorial Institute P.O. Box 999 Richland, Washington 99352		10. PROGRAM ELEMENT, PROJECT, TASK AREA & WORK UNIT NUMBERS PRON M1-4-A1555-01-M1-MS AMS Code 3297.06.7501
11. CONTROLLING OFFICE NAME AND ADDRESS CDR, Rock Island Arsenal GEN Thomas J. Rodman Laboratory Rock Island, Illinois 61201		12. REPORT DATE October 1975
		13. NUMBER OF PAGES 41
14. MONITORING AGENCY NAME & ADDRESS (if different from Controlling Office)		15. SECURITY CLASS. (of this report)  UNCLASSIFIED
		15a. DECLASSIFICATION/DOWNGRADING SCHEDULE
16. DISTRIBUTION STATEMENT (of this Report)  Approved for public release, distribution unlimited.		
17. DISTRIBUTION STATEMENT (of the abstract entered in Block 20, if different from Report)		
18. SUPPLEMENTARY NOTES		
19. KEY WORDS (Continue on reverse side if necessary and identify by block number)		
1. Sputter Deposition	3. Tungsten Coatings	
2. Coating on Gun Tubes	4. Chromium Coating	
20. ABSTRACT (Continue on reverse side if necessary and identify by block number)		
<p>This work was conducted to establish sputter deposition as a candidate production coating process for military items. Specifically two areas were evaluated -- deposition on internal bore surfaces of gun barrels and deposition of wear resistant coatings on external surfaces. The feasibility of sputter deposition on bore surfaces of 7.62mm gun tubes was studied using both a modified dc-triode scheme with tungsten targets centered on the gun</p>		

(over)

DD FORM 1 JAN 73 1473

EDITION OF 1 NOV 65 IS OBSOLETE

UNCLASSIFIED

SECURITY CLASSIFICATION OF THIS PAGE (When Data Entered)

tube axis and a dc-diode scheme with the plasma supported by thermally emitted electrons from a hot target/filament centered on the gun tube axis. Although the latter scheme gave better deposition characteristics, further refinements appear necessary before the method can be adapted as a production coating process. High quality chromium coatings were produced on 7076-T6 aluminum substrates in the work involving deposition on external surfaces. The wear test results indicate the sputter deposited chromium coatings exhibited superior substrate adherence and more uniform wear characteristics when compared to the electro-deposited chromium plating.

## FOREWORD

This report covers the work performed under MIPR M5-4-P0048-01-M5-W3 by R. H. Jones, R. W. Moss, E. D. McClanahan and H. L. Butts of the Battelle Pacific Northwest Laboratories. The work was conducted for the GEN Thomas J. Rodman Laboratory, Rock Island Arsenal, Rock Island, Illinois with W. T. Ebihara and A. Crowson as project engineers.

The contributions of the following people are gratefully acknowledged: R. F. Stratton and I. B. Mann for the gun barrel coating; E. L. McDonald for the chromium coating; J. E. Spasoff for the density and x-ray determination; R. Busch and N. Laegreid for their very helpful suggestions on materials and sputtering technology; and R. H. Beauchamp and D. H. Parks for metallography.

This work was authorized as part of the Manufacturing Methods and Technology Program of the U.S. Army Materiel Command and was administered by the U.S. Production Equipment Agency.

CONTENTS

	<u>Page</u>
DD FORM 1473 (Document Control Data R&D) . . . . .	i
FOREWORD . . . . .	iii
TABLE OF CONTENTS . . . . .	iv
LIST OF TABULAR DATA . . . . .	vi
LIST OF FIGURES . . . . .	vii
1.0 INTRODUCTION . . . . .	1
2.0 FEASIBILITY STUDY OF SPUTTER DEPOSITING TUNGSTEN ON THE BORE SURFACE OF 7.62mm GUN TUBES. . . . .	2
2.10 Procedure . . . . .	2
2.11 Characteristics of Sputtering Modes . . . . .	2
2.12 Identification of Process Variables . . . . .	2
2.13 Evaluation Techniques. . . . .	3
2.14 Cleaning Procedures . . . . .	3
2.20 Mode I Experiments . . . . .	3
2.21 Results. . . . .	3
2.22 Discussion . . . . .	4
2.23 Conclusions . . . . .	5
2.30 Mode II Experiments . . . . .	5
2.31 Results . . . . .	5
2.32 Discussion . . . . .	6
2.33 Conclusions . . . . .	8
3.0 CHROMIUM WEAR COATINGS . . . . .	8
3.10 Procedure . . . . .	8
3.20 The Effect of Substrate Temperature . . . . .	9
3.21 Results . . . . .	9
3.22 Discussion . . . . .	10

	<u>Page</u>
3.30 The Effect of Substrate Potential. . . . .	11
3.31 Results. . . . .	11
3.32 Discussion . . . . .	12
3.40 Some Other Features of Chromium Coatings . . . . .	13
3.41 Deposit Defects . . . . .	13
3.42 Fracture Behavior . . . . .	13
3.43 Conclusions. . . . .	13
4.0 SUMMARY AND RECOMMENDATIONS. . . . .	14
5.0 REFERENCES . . . . .	16
DISTRIBUTION. . . . .	35

LIST OF TABLES

	<u>Page</u>
Table I      Summary of Mode I Sputtering Experiments for the Deposition of Tungsten on the Bore Surface of 7.62mm Gun Tubes . . . . .	17
Table II     Summary of Mode II Sputtering Experiments for the Deposition of Tungsten on the Bore Surface of 7.62mm Gun Tubes . . . . .	18
Table III    Summary of Chromium Sputter Deposition Parameters and Properties . . . . .	19
Table IV     Chemistry of Sputtered Chromium Coatings and Target Material . . . . .	20

## LIST OF FIGURES

	<u>Page</u>
Figure 1	Schematics of Apparatus for Evaluating the Feasibility of Sputter Coating the Bore Surface of 7.62mm Gun Tubes . . . . . 21
Figure 2	Gun Barrel Sputtering Apparatus . . . . . 22
Figure 3	Photograph of 0.040 in. dia. Tungsten Target Material. . . . . 23
Figure 4	Measured Target Diameter vs. Position Within Gun Tube . . . . . 24
Figure 5	Measured Target Diameter vs. Position Within Gun Tube . . . . . 25
Figure 6	Optical Photomicrographs of Traverse Section of 7.62mm Gun Tube Showing Tungsten Deposit . . . . . 26
Figure 7	Scanning Electron Micrographs of Tungsten Deposit Removed from Muzzle End of 7.62mm Gun Tube . . . . . 27
Figure 8	X-ray Energy Spectrograph of Tungsten Deposit With Characteristic $L_{\alpha}$ and $L_{\beta}$ Energies for Tungsten Indicated . . . . . 28
Figure 9	Deposit Hardness and (220) Interplanar Spacings vs. Substrate Temperature for Sputter-Deposited Chromium. . . . . 29
Figure 10	Optical (OM) and Scanning Electron Micrographs (SEM) of Sputter-Deposited Chromium . . . . . 30
Figure 11	Scanning Electron Micrographs of Sputter-Deposited Chromium Growth Surface . . . . . 31
Figure 12	Optical (OM) and Scanning Electron (SEM) Micrographs of Sputter-Deposited Chromium Showing Some Growth Defects . . . . . 32
Figure 13	Scanning Electron Micrographs of Sputter-Deposited Chromium Fracture Surfaces . . . . . 33
Figure 14	Scanning Electron Micrograph of Deposit No. 2 Fracture Surface Showing Cleavage Planes . . . . . 34

## 1.0 INTRODUCTION

The service life of rapid-fire machine gun and automatic rifle components is often less than desired because of a general phenomenon called wear. In the case of gun barrels, rapid wear may be attributed to induced heating caused by combustion products and projectile/bore surface interaction. If this is in fact the case, wear could be reduced by a coating with either or both of the following properties:

- a. Retention of a high hardness level to temperatures of  $\sim 2000^{\circ}\text{F}$ ; e.g., the refractory metals and alloys or, to a lesser degree, the superalloys.
- b. A reduced coefficient of friction (relative to steel) with the copper-zinc jacketing material; e.g., metals immiscible with and not wet by copper-zinc.

The coatings would also require a very high degree of adherence. Receiver components which undergo sliding friction could also exhibit extended service lives with coatings possessing higher hardness and greater bond strength.

Sputter deposition offers the potential for producing the types of coatings discussed above. The process is capable of high deposition rates with a wide range of materials, and is characterized by a high level of adherence of the coating to the substrate. Numerically controlled, production level equipment has been developed.

The major objective of the program was to establish sputter deposition as a candidate production coating process for military items. Specifically the program consisted of two areas -- deposition on the internal bore surfaces of gun barrels, and deposition of wear resistant coatings on test coupons and small arms parts.

The objective in the gun barrel coating area was to determine the feasibility of applying satisfactory coatings on the internal surfaces of sub-10mm bore gun barrels. This was approached in two ways -- one, by adapting the conventional triode sputtering scheme to fit the 7.62mm bore by 20 in. long gun tube configuration provided. The other using a scheme where the filament and sputtering target functions were served by a rod centered on the axis of the gun tube. The feasibility study was carried out using tungsten targets.

The objective in the deposition of wear resistant coatings was to establish suitable process parameters for the application of chromium coatings to standard cylindrical wear test specimens.

## 2.0 FEASIBILITY STUDY OF SPUTTER DEPOSITING TUNGSTEN ON THE BORE SURFACE OF 7.62mm GUN TUBES

### 2.10 Procedure

#### 2.11 Characteristics of Sputtering Modes

The feasibility of sputter depositing tungsten on the bore surfaces of 7.62mm gun tubes has been studied with two experimental approaches illustrated in Figure 1, and hereafter referred to as Modes I and II. A photograph of the assembled gun tube sputtering apparatus is shown in Figure 2.

The basis of Mode I was the establishment of an ionized plasma within a chamber at one end of the gun tube with an anode at the opposing end. A negative potential applied to a tungsten target centered within the gun tube attracted the positively ionized gas atoms; thereby sputtering the tungsten target atoms.

The basis of Mode II was the thermal emission of electrons from a hot target centered on the bore axis; the acceleration of these electrons towards the barrel to create ions; the acceleration of the positively charged ions towards the target to sputter the target atoms; and finally the deposition of these atoms on the bore surface. A tungsten filament must be heated above 3600°F before a practical quantity of electrons are thermionically emitted; however, emission then depends exponentially on temperature so that small changes in temperature produce large changes in emission.

#### 2.12 Identification of Process Variables

The independent variables studied in Mode I were voltage gradient in the tube as controlled by upper anode potential, gas pressure and type, pressure gradient and lower plasma current. Apparatus modifications were made as problems were identified. The independent variables studied in Mode II were the gas pressure, target voltage and filament current. The filament current is defined as the current used to resistively heat the target while the target current is the current flow between the target and the barrel which is an anode. The dependent variables in both cases were the target current, weight and diameter change of the target and target appearance. The appearance of an ion bombarded tungsten surface is considerably different than the chemically etched surface after target cleaning. The upper anode current was also a dependent variable in Mode I.

### 2.13 Evaluation Techniques

Optical metallography of transverse and longitudinal sections was performed when the data indicated tungsten had been sputtered onto the gun tube. Flakes of this deposit were also examined with an ETEC Autoscan Microscope operated at 20 kV in the secondary electron imaging mode while chemical analysis of the deposit was performed with a Kevex X-Ray Energy Spectrometer. A tin target was used with a potential of 50 kV and a current of 40 ma.

### 2.14 Cleaning Procedures

The tungsten targets were chemically etched in a 5% solution of HF in water for 15 min., rinsed with reagent grade methanol and air dried. When a new gun tube was assembled, the following cleaning procedure and presputtering procedure was used:

- a. Rinse with reagent grade alcohol while scrubbing with nylon brush.
- b. Rinse with reagent grade alcohol.
- c. Hot air dry.
- d. Assemble and evacuate.
- e. Bakeout --
  - (1) Mode I: Heat chamber with external heat source - 2 hours.
  - (2) Mode II: Heat gun tube with filament.

### 2.20 Mode I Experiments

#### 2.21 Results

A summary of the meaningful Mode I experiments is presented in Table I. These results are values at which an upper anode current and a target current were detected. For a given experiment, the upper gas pressure and anode potential were separately varied in efforts to find conditions which resulted in an upper anode current. A tungsten emitter, which protruded into the upper anode chamber, was excited with a high voltage by touching it with a Tesla coil. This procedure was used to aid ionization in the upper chamber.

An upper anode current was achieved only when the gas was metered into the upper chamber and the pressure in this chamber exceeded 0.1 torr. The four experiments summarized in Table I had this pressure dependence in common with variable upper anode current, lower anode current, pressure gradient and type of gas having little effect on the performance of the apparatus. The upper anode current was reduced from 3 amps to 1 amp by placing a resistance in series with the upper anode and ground. The lower pressure was raised in experiment No. 4 by metering krypton into the bottom and top chambers simultaneously. A higher pressure in the lower chamber was not possible because of equipment limitations.

The target weight losses were proportional to the total ion flux bombarding the target which is given by the product amps x hrs. These products are very qualitative since the target current was very rough with several on-off cycles per experiment. Shorting between the target and barrel occurred because of electrical arcing and mechanical vibrations which caused the long tungsten target to vibrate sufficiently to make contact. Target fracture caused experiments to be terminated even though the target was stressed less than 1000 psi. The target surfaces did not have the normal appearance of a sputtered target surface as they had a rough appearance with large spikes protruding radially outward. A photograph showing these spikes on the target from experiment No. 3 is shown in Figure 3b. Borescope examination of the bore surface revealed a very rough appearing deposit over the bore length equal to the rough-appearing target length. Based on the target diameter change and the target surface appearance, tungsten was removed from the target only over the upper 10 - 12 in. and 1 - 2 in. near the muzzle end. The target diameter vs. position within the barrel is plotted in Figure 4 for experiment Nos. 3, 4, and 5. The initial target diameters were consistently  $0.040 \pm 0.0001$  in.

## 2.22 Discussion

There are two possible explanations for the tungsten removal from the target at the chamber end while none was removed within the lower section of the gun tube. One explanation is that a plasma existed within the gun tube but it had nonuniform density because of the pressure gradient within the gun tube. This mechanism is supported by experiment No. 4 where the smallest pressure gradient resulted in tungsten removal over the longest length of target. Another explanation is the conductance of electrons through the barrel in favor of the bore, the emission of these electrons by ion bombardment in the upper anode chamber and the flow of these electrons to the upper anode. The pressure gradient then causes ions to flow down the gun tube and bombard the target over its upper portion. Because an upper anode current was not achieved without ionization produced by exciting the tungsten emitter, it was concluded that a glow discharge existed between the chamber end of the barrel and the upper anode supported by electrons conducted up the barrel. This was verified by the elimination of the upper anode current when the lower plasma was turned off.

## 2.23 Conclusions

It was concluded that the Mode I scheme for depositing tungsten on the bore surface of a 7.62mm gun tube showed little potential for producing a uniform deposit. The discharge conditions which existed in the upper anode chamber could possibly be solved by electrically insulating the chamber end of the barrel from the upper anode; however, there was little evidence that electrons could be accelerated up a 7.62mm diameter by 20 in. long tube. The length and  $D^2$  dependence of this technique also suggest that further efforts to produce a plasma within a small diameter, long tube would not be beneficial.

## 2.30 Mode II Experiments

### 2.31 Results

A summary of the meaningful Mode II experiments is presented in Table II. Glow discharge conditions existed between the target and the barrel at a pressure of  $380 \times 10^{-3}$  torr and a potential of 650 volts, and also at  $250 \times 10^{-3}$  torr and 500 volts. The glow discharge condition was verified by the continuation of a target current with the filament current removed, as in experiment Nos. 8 and 12. The glow discharge persisted in the chamber in experiment No. 8 and outside the barrel at the muzzle end in experiment No. 10.

Experimental verification of the feasibility of sputtering tungsten on the bore surface of a 7.62mm gun tube was obtained in experiment No. 10. A krypton pressure of  $250 \times 10^{-3}$  torr, target potential of -250 and filament current of 43 amps resulted in a target current of 3 amps. Sputtering proceeded for approximately 1 hour to give 3 amp-hrs of ion bombardment and a target mass change of 0.786 g. Target fracture caused the experiment to be terminated. The target mass change due to thermal evaporation of volatile compounds and possibly tungsten was found to be 0.110 g which was determined by maintaining the conditions of experiment No. 10 but without a target potential. No diameter or surface change was found with these conditions, as the data for experiment No. 11 indicates. The plot of target diameter vs. position within the gun tube, shown in Figure 5, illustrates the uniform metal removal over the entire length in experiment No. 10. The large diameter reduction within the chamber was the result of plastic strain within the region of fracture. Further experimental verification was obtained with experiment No. 17; however, the target was not as uniformly sputtered as in experiment No. 10.

In an effort to extend the duration and therefore the amount of deposit per experiment, a 0.050 in. diameter tungsten target was substituted for the 0.040 in. diameter tungsten target in experiment No. 13. The experiment was terminated by a target-barrel short because 60 - 70 amps of

filament current are required to heat a 0.050 in. diameter tungsten wire to the same temperature that 40 - 45 amps will heat a 0.040 in. diameter wire: the target loading and aligning fixture which must also carry the filament current was not adequate for the 0.050 in. diameter target. Rather than redesign the loading fixture at a late date in the program, it was decided that reasonable reproduction of experiment No. 10 would be an adequate demonstration of feasibility. Experiment No. 17 provided this verification.

Through the first 17 experiments the same barrel was used in order to save time and conserve funding. Metallographic sections were taken from this barrel even though it had a complex history. Optical photomicrographs of sections near the muzzle and the chamber are shown in Figure 6. The layered structure resulted from deposition occurring over successive experiments, while the lack of bonding was partially caused by lack of cleaning between experiments. Ion etching is not achievable at present with the Mode II scheme. Improved bonding between barrel and deposit resulted near the chamber end which may have resulted from higher barrel temperatures at this location. Although the thermocouples, which were placed along the barrel, failed in an early experiment there was one instance when the chamber end of the barrel was approximately 2000°F, as judged by its color. This high temperature resulted from the target contacting the barrel and was not a typical condition.

Scanning electron micrographs of tungsten deposit removed from the muzzle end of the barrel are shown in Figure 7. A cross-sectional view of a fracture surface is shown in Figure 7a, where the growth structure of the deposit are very characteristic of sputter deposited material. Verification that the deposit was tungsten was obtained by x-ray energy spectroscopy. A photograph of the resulting spectrograph is shown in Figure 8 with  $L_{\alpha}$ ,  $L_{\alpha_2}$ ,  $L_{\beta}$ , and  $L_{\beta_2}$  energy levels of tungsten indicated above it. The peaks shown on the spectrograph are the  $L_{\alpha_1}$  and  $L_{\alpha_2}$  of tungsten combined at 8.4 eV and the  $L_{\beta_1}$  at 9.65 eV, and  $L_{\beta_2}$  at 9.9 eV.

### 2.32 Discussion

Discussion of Mode II sputtering experiments will be limited primarily to experiment No. 10 and No. 17 because of the relative success obtained with an applied target voltage of -250 V, 150 to 250 x 10<sup>-3</sup> torr gas pressure and 40 - 43 amps of filament current. While the gun tube sputtering apparatus was designed to operate in both modes, it soon became apparent that some minor changes were needed for Mode II. Since the target temperature and electron emission are fairly uniform along the target length, ionization and ion bombardment can occur over the entire length. In fact, ionization is favored at the longer anode-target gaps which occur outside of the gun tube;

therefore, it was not surprising to find target sputtering rates were highest within the chambers and near the muzzle end. Efforts were made to electrically isolate the target extremities from the anode with MgO tubing but thermal evaporation was sufficient to allow a tungsten coating to be formed on the MgO surface. This coating was also adequate to cause electrical contact to the gun tube and the breakdown of electrical isolation. Also, the target surface had a dark appearance within this region which was attributed to a chemical reaction between the tungsten and volatile compound within the MgO. Metallic sleeves and shields were constructed such that the target is contained within a constant diameter over its entire length; however, the apparatus was not operated with them.

Target alignment, tension and current contact are the key elements on which the reproducibility and reliability of this scheme depend. Alignment is maintained by the target loading mechanism which is aligned by four guide pins. These pins help maintain alignment with the target thermal expansion of 1 - 2 cm. The target tension was maintained by two stainless steel springs with spring constants of 2 mg/cm which resulted in 8 mg of load at room temperature and approximately 4 mg at 3600°F. Some target tension is necessary at the operating temperature because of plasma instabilities and apparatus vibrations; however, this tension also contributes to target failure. A local reduction in target diameter can cause an accelerated reduction to occur because the target becomes locally hotter and therefore a locally higher stress and strain rate. Also, a locally greater plasma density would be created because of the greater electron emission resulting in a locally greater sputtering rate. A larger diameter target may reduce these problems; however, an improved current contact capable of handling 70 - 80 amps without unnecessary side or axial loads on the target is necessary. Presently, the current is conducted through the tension springs but this raises their temperature and lowers their stiffness which allows target-barrel contact to occur and therefore an electrical short between anode and target. Perhaps a lever arm could be used to apply the load and the current contact through a liquid mercury pool within the chamber; however, this poses loading and plasma contamination problems. Another possibility is to apply the tension externally through a sliding seal and make electrical contact on this rod. The difference between static and dynamic friction of the seal and the small designed tension is a possible problem with this approach.

Ion etching of the substrate cannot be performed in the usual manner with the Mode II scheme. Conditions under which a plasma could be generated with the barrel as target and the tungsten as anode may exist but these were not investigated. Also, it may be possible to ion etch using the Mode I scheme; however, it would be difficult to etch the entire length.

### 2.33 Conclusions

Successful demonstration of the feasibility of sputter depositing tungsten on the bore surface of 7.62mm gun tubes was achieved using the Mode II scheme with a krypton gas pressure of  $250 \times 10^{-3}$  torr, a target voltage of -250 V and a filament current of 40 - 43 amps. A uniform target reduction of 0.0025 cm resulted which would correspond to a 0.000375 cm thick deposit. A total deposit thickness of 0.00125 cm was obtained from a series of experiments using the same gun tube. It was concluded that the Mode II scheme showed sufficient promise to warrant further evaluation along with improved target alignment, load application, high current contact and shielding.

## 3.0 CHROMIUM WEAR COATINGS

### 3.10 Procedure

Chromium coatings on 1.375 in. diameter hollow cylinders of 7075-T6 aluminum were produced by high-rate sputter deposition in a dc-triode system. The aluminum cylinders were water cooled and rotated at 40 revolutions per minute above a 4 in. diameter flat Marz Grade lochrome\* sputtering target obtained from Materials Research Corporation. A substrate-to-target spacing of 0.375 in. was used for all deposits. Prior to assembly, the substrates were vapor degreased, rinsed with trichloroethylene and methanol, ultrasonically cleaned for 15 min. in water, rinsed with methanol and air dried. The substrates were ion etched at a potential of -100 V for 5 min. in a plasma of krypton gas at a pressure of  $3 \times 10^{-3}$  torr prior to sputter depositing the chromium. Chromium deposits were made with target potentials of -1500 V and -2000 V, substrate potentials of -30 V (floating) and -50 V (biased), substrate temperatures of 68°F and 140°F and deposition rates of 0.3 to 0.7 mils/hr.

Structural evaluation of the chromium deposits was done by x-ray diffraction, optical metallography and scanning electron microscopy (SEM) of fracture and growth surfaces. Copper radiation produced by 35 kV electrons at 20 ma, filtered through nickel and collimated with 1° slits was used to study the crystalline structure and texture of the chromium deposits. Optical metallography was performed on transverse sections for the purpose of studying grain size and shape, growth defects and deposit thickness. The grain size and shape was also studied by SEM of fracture surfaces while growth features were also studied by SEM of the chromium surface. An ETEC Autoscan Microscope was used for the SEM work with a beam potential of 20 kV and secondary electrons for image

\*Registered trademark of Chromalloy American Corp.

formation. Both trace impurities and krypton content of powdered chromium were analyzed with a Kevex X-Ray Energy Spectrometer operated at 42.5 kV and 10 ma. The  $K_{\alpha}$  peak height above background of krypton relative to the  $K_{\beta}$  chromium peak was used as a measure of krypton content.

The microhardness of the chromium and the aluminum substrate was measured on transverse sections. Both diamond pyramid and Knoop indentors with 100 g and 200 g loads were used to obtain the mid-thickness hardness of the chromium. Density measurements of the chromium coatings, after the substrate had been dissolved in a solution of KOH in  $H_2O$ , were made by the displacement method in a microdensity apparatus. A fluorochemical, perfluorotributylamine, was used as the displacement fluid. Wear tests of sputter deposited and electrodeposited chromium on cylindrical specimens were performed at Rock Island Arsenal. Wear rates were measured as a function load applied to a tungsten carbide pad under oscillating contact conditions (Alpha LFW-1 test).

### 3.20 The Effect of Substrate Temperature

#### 3.21 Results

The hardness of sputter deposited chromium exhibited similar temperature dependence when the substrate was floating and biased; although, the deposit was harder when a bias was applied. The diamond pyramid (DPH) and Knoop hardnesses (KHN) of chromium sputter deposited on rotating cylindrical and flat substrates as a function of substrate temperature as shown in Figure 9. At 752°F, little hardness difference was found for the floating and biased conditions while a difference of 100 DPH existed at 68°F. For most materials the DPH and KHN are equivalent, but for the chromium deposits a considerable difference existed. Since the Knoop indenter is rhombic in shape with one diagonal seven times the length of the other and the hardness measurements were made on transverse sections with the long diagonal parallel to the deposit plane, the KHN should be the better measure of deposit hardness. However, the KHN values were less reliable than the DPH values, because of the scatter caused by the difficulty in measuring its diagonal length. The DPH values suggest a maximum at 140°F for the chromium deposited with a -50 V potential; however, the KHN values and the DPH values for a -30 V substrate potential suggest a continuously decreasing hardness with increasing temperature. In coincidence with the observed hardness changes with temperature, the crystal lattice parameter decreased with temperature, as shown in Figure 9, until at 302°F it equaled the ASTM value for bulk chromium. The lattice parameter was independent of substrate potential for -30 V and -50 V potentials. While grain size of chromium deposited with a bias was unresolvable, a grain size difference was observed for substrate temperatures of 68°F and 140°F with a floating substrate potential. A quantitative comparison was complicated by the conical grain shape and

the poor grain boundary resolution of the lower temperature deposit; however, the largest grain diameters at mid-thickness were 2  $\mu\text{m}$  and 6  $\mu\text{m}$  for these two temperatures, respectively. The grain size difference for these two deposits is readily seen in the optical and SEM micrographs of Figure 10. There was some evidence of twinning in deposit No. 4, and by the observed lack of growth interfaces in the twins, it was concluded that they are post-deposition mechanical twins. In all cases, the grains were conical or columnar-shaped with a (110) fiber texture perpendicular to the deposit plane. It has been shown by Patten and McClanahan<sup>1</sup> that the columnar grain shape persists up to a substrate temperature of 717°F for sputter deposited chromium but the preferred growth direction is replaced by a random grain orientation in the deposit plane.

The substrate temperature was found to have little effect on the deposit density, trapped krypton content or trace impurities, as the data in Tables III and IV illustrate. A slight downward shift in the krypton content with increasing substrate temperature was noted; however, the shift was not significant enough to support a conclusion. Also, a high potassium content was observed in deposit Nos. 2 and 5 which was attributed to the ceramic mortar and pestle used to grind the deposit.

### 3.22 Discussion

A number of possible mechanisms can be postulated to explain the hardness dependence of sputter deposited chromium on substrate temperature. Included in this list of mechanisms are: trapped gas content such as krypton; grain size; crystalline defect structure such as line defects and vacancies; and intergrain porosity. Intergrain porosity may account for the density of sputter deposited chromium being less than bulk chromium and for its dependence on substrate potential, but not the hardness dependence on temperature since the density was independent of temperature at a -30 V substrate potential.

Line broadening occurs with cold worked metals and alloys because of nonuniform strain between grains and a high dislocation density fragments the grains into subgrains. Line broadening is accompanied by resolution loss of the  $K_{\alpha}$  doublet. Both line broadening and lack of a resolved  $K_{\alpha}$  doublet were characteristics of the x-ray diffraction pattern of all the sputter deposited chromium. A change in the line breadth with substrate temperature was not observed while a line shift which depended on substrate temperature was observed. This line shift which indicated a lattice expansion could be explained by krypton trapped in the chromium lattice. While the total krypton content was only slightly dependent on temperature, the concentration of krypton in solution could have diminished with higher substrate temperature. A grain size change with increasing temperature was

<sup>1</sup> J.W. Patten and E.D. McClanahan, J. Appl. Phys., Vol. 43, No. 11 (1972), p. 4811

shown for a substrate potential of -30 V and therefore it was concluded that a grain size effect was partially responsible for the temperature dependence of the hardness.

### 3.30 The Effect of Substrate Potential

#### 3.31 Results

A hardness increase of 100 DPH resulted from a substrate potential increase of -20 V for chromium sputter deposited on a rotating cylindrical substrate at 68°F. A similar increase was observed in earlier Battelle-Northwest work for chromium deposited on flat substrates at 68°F. Agreement between the hardness of chromium deposited on rotating cylindrical and flat substrates at 68°F suggests that the hardness of chromium deposited on rotating cylindrical substrates at 752°F would also be independent of small substrate potential changes.

Accompanying and probably accounting for the hardness dependence on substrate potential were changes in grain size, krypton content and density of the chromium deposits. The grain structure of chromium deposited on rotating cylindrical deposits at 68°F and 140°F and a substrate potential of -50 V was not satisfactorily resolved by optical metallography or scanning electron microscopy of fracture surfaces. Therefore, a quantitative comparison of grain sizes with substrate potential was not possible; however, a qualitative grain size comparison can be made by comparing the scanning electron micrographs of fracture surfaces shown in Figure 10. It is apparent from these photographs that both the length and diameter of the chromium grains have been reduced; the diameter by at least a factor of 10 and the length perhaps by more. Also, the free growth surfaces were altered from nonparallel to the substrate surface, for a substrate potential of -30 V, Figures 10 a-d; to parallel for -50 V, Figures 10e and f. The nonparallel growth surfaces can be seen in Figures 10a-d and 11, while the parallel growth surfaces are shown in Figure 10e and f. Surface reflectivities of dull and bright accompanied these growth features, respectively.

A comparison of the relative intensities of the above background  $K_{\alpha}$  peak of krypton to the  $K_{\beta 1}$  peak of chromium as determined by x-ray energy spectroscopy is made in Table III. These results suggest a lower krypton content for the chromium deposited with a -50 V substrate potential as compared to a -30 V potential. This trend occurred at substrate temperatures of 68°F and 140°F. Winters and Kay<sup>2</sup> observed a similar effect for argon concentration in nickel where the concentration decreased with small negative potentials because of the high sputtering yield of adsorbed argon, and increased at larger negative potentials because the ions were implanted within the nickel crystal lattice.

<sup>2</sup> H.F. Winters and E. Kay, J. Appl. Phys., 38, (1967), 3928.

Deposition of chromium with a -50 V substrate potential at 68°F resulted in a density of 7.10 g/cm<sup>3</sup> as compared to 7.19 g/cm<sup>3</sup> for bulk chromium. Deposition at -30 V potential, and 140°F with -50 V potential resulted in lower densities but still within 10% of bulk density, as the data listed in Table III indicate. It is expected that deposit Nos. 5 and 6 had densities close to deposit No. 1 but their brittleness inhibited density measurements.

### 3.32 Discussion

Modifications in growth morphology with the application of a negative substrate potential has been observed by other workers;<sup>1,3</sup> however the mechanisms involved have not been clearly established. Mattox and Kominiak<sup>3</sup> attributed the growth habit modification and densification of tantalum deposits to resputtering of the deposit surface during growth, while Patten and McClanahan<sup>1</sup> observed a grain refinement with increased substrate bias. An applied negative bias can affect the deposition process by altering plasma characteristics, thermal effects, resputtering, alterations in the terrace-ledge-kink growth mode and nucleation rate. At the low biases used in the present work, the surrounding plasma would be little affected and thermal effects were minimal. Resputtering was either non-existent, based on deposition rates, or very selective. Both the growth mode and the nucleation rate were altered, in some way, since the grain shape and length were altered.

It is suggested that the highly textured chromium was cathodically polished at the low substrate potentials. The strong crystal-line texture resulted in equal resputtering rates for all the grains while the fine grain size made the etched grain boundaries unresolvable. A floating substrate potential of -30 V was apparently below the sputtering yield for chromium bombarded with krypton ions while a -50 V potential was above the yield. Without the resputtering effect, the growth planes were nonparallel to the deposit plane which favored a conical grain shape. An increasing grain diameter with deposit thickness resulted from this conical grain shape.

Resputtering eliminated the nonparallel growth surfaces in favor of parallel ones which resulted in cylindrical chromium grains and a constant grain diameter with deposit thickness. The elimination of nonparallel growth surfaces may have been due to the higher sputtering yield of these planes either for crystallographic reasons or because BCC metals exhibit higher sputtering yields for nonperpendicular than perpendicular surfaces.<sup>4</sup>

<sup>1</sup> J.W. Patten and E.D. McClanahan, J. Appl. Phys., Vol. 43, No. 11 (1972), p. 4811

<sup>3</sup> D.M. Mattox, J. Vac. Sci. & Tech., Vol. 9 (1971), p. 528.

<sup>4</sup> G. Wehner, Sci. and Tech., Sept. 1968, 32.

### 3.40 Some Other Features of Chromium Coatings

#### 3.41 Deposit Defects

Inclusions in the extruded 7075-T6 aluminum alloy were extracted by ion etching which resulted in surface grooves in the longitudinal, linear defects in the chromium coatings, as shown in Figures 12a, b. Successive sections followed by metallographic polishing and examination were used to verify that the defects shown in Figure 12a were linear. The SEM micrograph of the chromium surface shows the replication of the substrate defect by the chromium. These defects were eliminated by reducing the current density during ion etching.

The presence of particulates on the substrate surface cause the formation of growth defects, such as the ones shown in Figures 12c, d. Careful cleaning and handling of the substrates prior to assembly within the sputtering chamber, helps to minimize the number of growth defects.

#### 3.42 Fracture Behavior

Fracture surfaces perpendicular to the deposit plane of the chromium were generated by partially sectioning the substrate followed by an applied bending stress. Scanning electron micrographs of some fracture surfaces are shown in Figure 13. The most noteworthy features of these fractures were lack of coating/substrate delamination while they did indicate a variable degree of delamination within the deposit. Deposit Nos. 1 and 6 showed the least delamination, with somewhat more in the others. When the substrate is ion etched prior to deposition, some of the sputtered aluminum deposited on the chromium target and was the first material to be deposited on the substrate. This Cr-Al alloy layer can be seen in the fracture surface of deposit No. 1 shown in Figure 13d.

Besides delamination, the chromium fractured by an apparent intergranular fracture and a cleavage fracture of the (100) planes. Examples of the intergranular and cleavage fractures are shown in Figure 14.

#### 3.43 Conclusions

The structure, chemical composition and properties of 0.005 cm thick chromium deposits produced by high-rate sputter deposition were found to depend on substrate temperature and potential with little dependency on target voltage and deposition rate. Both deposit hardness and crystal lattice parameter decreased with increasing substrate temperature. It was concluded that a decreasing crystalline defect density could account for both the hardness and lattice parameter changes. This conclusion was supported by the independence of the density, krypton content and trace impurities in the deposit on substrate temperature. Deposit densities within 10% of that for bulk chromium were obtained with a floating substrate potential (-30 V) and substrate temperatures of 68°F and 140°F.

Increasing the substrate bias potential to -50 V during deposition altered both the growth morphology and the krypton content of the chromium, but had little effect on the lattice parameter. Columnar grains with a (110) fiber axis normal to the deposit plane resulted from all depositions in this work; however, their length and diameter were markedly reduced by increasing the substrate bias. A hardness increase of 150 KHN accompanied the bias-induced grain refinement. Bombardment of the deposit during deposition with low energy krypton ions resulted in less trapped krypton in the deposit in comparison to the floating substrate case. Resputtering of trapped krypton would account for this observation.

When the substrate was at a floating potential, only low index growth planes were present on the surface, while only (110) growth planes were present when the substrate was biased. The low index growth planes were probably the (100) plane because of their 45° angular relationship with the (110) fiber axis. Surface reflectivities of dull matte and bright accompanied these surface growth features.

Grain refinement resulted from this altered growth mechanism by the elimination of competitive grain growth with applied substrate bias. Competitive grain growth resulted from conical-shaped grains and therefore an increasing grain size with deposit thickness. Simple cylindrical-shaped grains which remained constant in diameter with deposit thickness resulted when the substrate was biased. A close relationship between the nucleation rate on the substrate and the final grain size may exist when this type of growth occurs.

#### 4.0 SUMMARY AND RECOMMENDATIONS

The feasibility of sputter depositing tungsten on the bore surface of 7.62mm gun tubes has been studied using both a modified dc-triode scheme with the target centered on the gun tube axis, and a dc-diode scheme with the plasma supported by thermally emitted electrons from a hot target/filament centered on the gun tube axis. A low quality deposit over one-half the gun tube length and no deposit over the remainder was obtained with the modified dc-triode scheme while a good quality deposit over the entire length was obtained with the modified dc-diode scheme. It was concluded that sufficient proof of coating feasibility was shown with the modified dc-diode scheme to warrant further evaluation. This effort should be directed towards improved reproducibility by modifications of the target aligning and tension mechanism, design and development of a current contact to allow larger diameter targets to be used and investigation of schemes to ion etch the gun tube surface.

Additional work on ion etching is required to establish the limiting relationship between the ability to ion etch the barrel ID and length. Although ion etching is considered to be an important factor in promoting good adherence, research concerning determination of its absolute necessity with the respect to coated barrel performance may lead to alternate considerations; e.g., other cleaning methods should be investigated to determine whether adequate bonding could be obtained without ion etching. With respect to the present technological position, it would then be possible to ion etch and coat a barrel having 3/4 inch ID.

High quality chromium coatings were produced on 7076-T6 cylindrical substrates. Cylindrical wear specimens with chromium coatings applied with six different sputtering conditions were sent to Rock Island Arsenal for testing. The results of these tests indicated the sputter deposited chromium coatings exhibited superior substrate adherence when compared to electro-deposited chromium and roughly equivalent wear rates although the sputtered chromium was softer. The results of this evaluation will be presented in a forthcoming report from Rock Island Arsenal. The hardness, structure and chemical composition of the coatings were determined. A maximum diamond pyramid hardness of 800 kg/mm<sup>2</sup> was obtained with a substrate temperature of 60°C, substrate potential of -50 V and target potential -1500 V.

## 5.0 REFERENCES

1. J.W. Patten and E.D. McClanahan, J. Appl. Phys., Vol. 43, No. 11 (1972), p. 4811.
2. H.F. Winters and E. Kay, J. Appl. Phys., 38, (1967), 3928.
3. D.M. Mattox, J. Vac. Sci. & Tech, Vol. 9 (1971), p. 528.
4. G. Wehner, Sci. and Tech., Sept. 1968, 32.

TABLE I  
Summary of Mode I Sputtering Experiments for the Deposition of  
Tungsten on the Bore Surface of 7.6 mm Gun Tubes

Exp. No.	Gas	Upper Pressure $10^{-3}$ torr	Lower Pressure $10^{-3}$ torr	$\Delta$ Pressure $10^{-3}$ torr	Lower Anode Volts	Lower Anode Current Amps	Applied Upper Anode Volts	Upper Anode Current Amps	Target Volts	Target Current Amps	Target Amp-Hrs	Target Wt. Loss g	Max. Target Dia. Chg in.	Target Appearance
1	Kr	150	4.2	146	65	3.2	300	3.0	-500	0.1	0.04	0.08	0.0003	Dark Gray
3	Kr	110	5.0	105	64	21	500	1.1	-500	0.4	0.11	0.82	0.004	Upper 10-in Spikes, Rest Unchanged
4	Kr	110	22	88	58	20	500	1.0	-300	0.32	0.10	1.03	0.010	Same as No. 3
5	Ar	140	8	132	65	17	500	1.0	-300	0.38	0.04	0.28	0.009	Same as No. 3

TABLE II

Summary of Mode II Sputtering Experiments for the  
Deposition of Tungsten on the Bore Surface of 7.6 mm Gun Tubes

Exp. No.	Pressure $10^{-3}$ torr	Filament Current Amps	Applied Target Voltage	Target Current Amps	Target Amp-hrs	Target Mass Loss g	Maximum Target Dia. Change, in.	Target Surface	Comments
8	380	22	-650	0.085	0.035	0.44	0.016	Very local reduction	Diameter change due to sputtering and plastic strain from alignment tension
10	250	43	-250	3.0	~ 3.0	0.786	0.0012 0.004- fract.	Bright, ion etched over length	Very positive results--had bright ion etched appearance over its entire length
11	250	43	--	--	--	0.110	0	Unchanged	Weight change due to volatile compounds such as solvents
12	250	40	-500	1.7	0.2	--	--	Mat'l removed nozzle end	Glow discharge condition verified by target current with zero filament current
13	270	70	-250	1.5	0.5	--	--	0.050 dia. target	Target shorted
16	250	30 - 40	-250*	1.0-1.5	0.4	0.5	0.013		Diameter change from strain and sputtering
17	150	30 - 40	-250*	1.5	4.2	1.26	0.0005 0.015- fract.	Bright, ion etched	Supports conclusion about feasibility from Exp. No. 10

\*Measured voltages with target current: Exp. 16 -70 V, Exp. 17 -120 V.

TABLE III

Summary of Chromium Sputter Deposition  
Parameters and Properties

Deposit	Substrate Temp °F	Substrate Potential V	Target Potential V	Deposition Rate mils/hr*	Deposit Hardness DPH	Relative Krypton Intensity**	Density g/cm <sup>3</sup>
1	68	-50	-1500	0.6	711 <sup>+21</sup> -34	$1.25 \times 10^{-3}$	7.10
2	68	Floating ~ -30	-1500	0.6	606 <sup>+71</sup> -34	$1.90 \times 10^{-3}$	6.52
3	140	-50	-1500	0.6	811 <sup>+25</sup> -36	$1.20 \times 10^{-3}$	6.67
4	140	Floating ~ -30	-1500	0.5	531 <sup>+14</sup> -18	$1.77 \times 10^{-3}$	6.60
5	68	-50	-2000	0.7	754 <sup>+20</sup> -44	$1.48 \times 10^{-3}$	
6	68	-50	-1500	0.3	764 <sup>+13</sup> -11	$1.19 \times 10^{-3}$	

\*Deposition rate based on radial buildup.

\*\* $I_{K_{\alpha}}(\text{Kr})/I_{K_{\beta_1}}(\text{Cr})$

TABLE IV  
Chemistry of Sputtered Chromium  
Coatings and Target Material \*

Specimen	Deposit							
	Ag $L_{\alpha}$	K $K_{\alpha}$	Ca $K_{\alpha}$	Fe $K_{\alpha}$	Ni $K_{\alpha}$	Cu $K_{\alpha}$	Zn $K_{\alpha}$	Ta $L_{\alpha}$
Target	17	-	56	12	9	22	12	50
1	23	-	56	17	-	22	12	35
2	23	150	68	22	-	45	11	45
3	23	50	56	22	5	45	39	39
4	11	22	56	22	5	79	51	45
5	22	145	68	22	11	79	56	34
6	45	11	56	22	8	62	11	22

\*X-ray peak intensity values permitting specimen-to-specimen comparison.

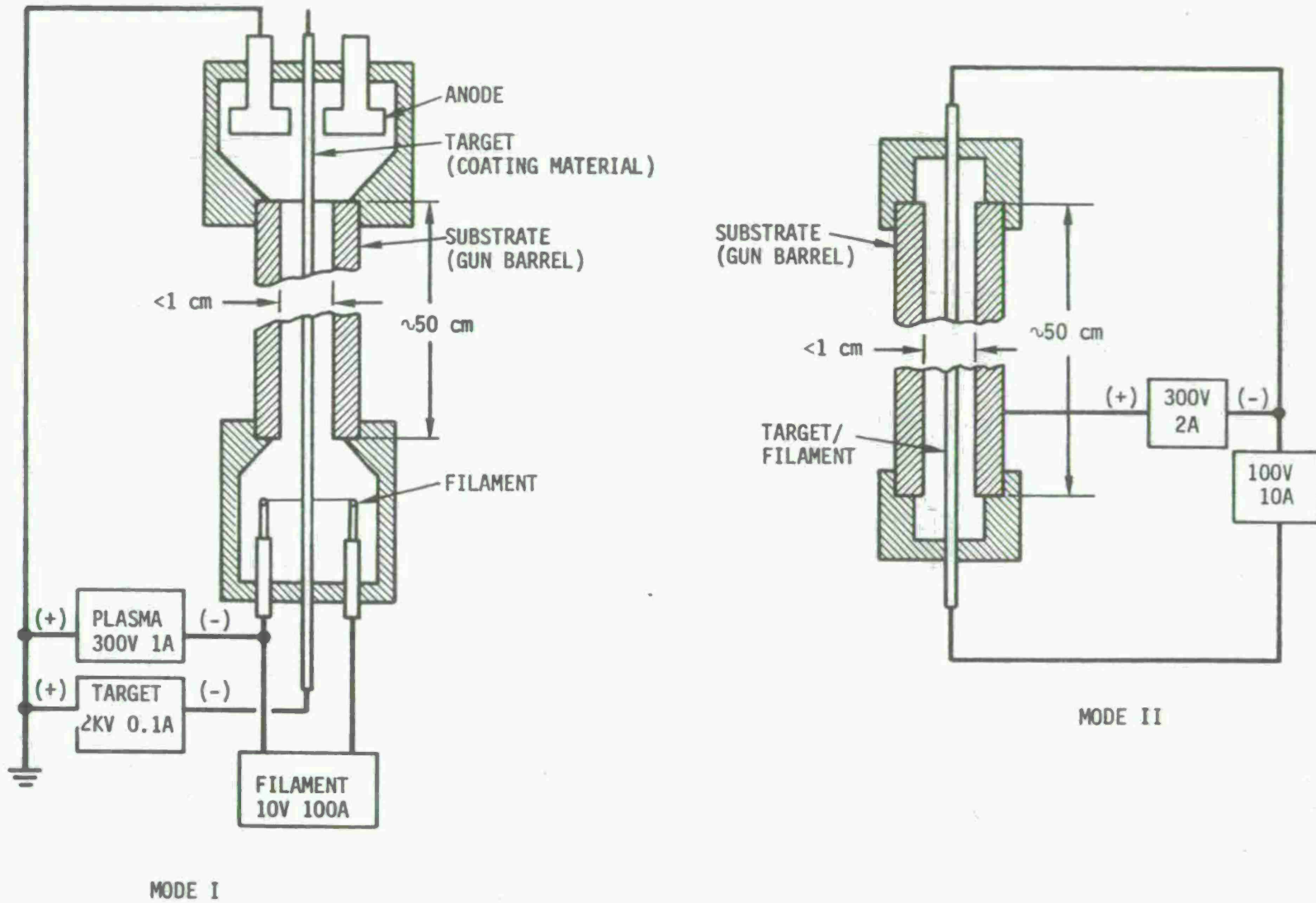
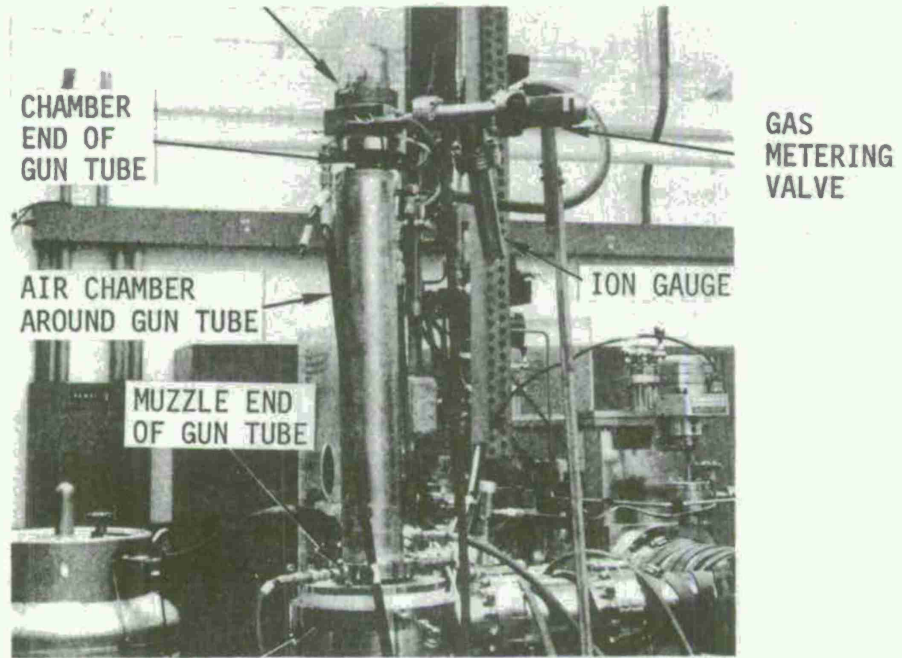


FIGURE 1. Schematics of apparatus for evaluating the feasibility of sputter coating the bore surface of 7.6 mm gun tubes.

TUNGSTEN TARGET  
ALIGNMENT AND  
LOADING



LOWER PLASMA  
CHAMBER

FIGURE 2. Gun barrel sputtering apparatus.



(a)

As-received.



(b)

Spikes on surface as in experiments No. 3, 4 & 5.



(c)

Ion-etched surface as in experiments No. 10 & 17.

FIGURE 3. Photograph of 0.040 in. dia. tungsten target material. 10X

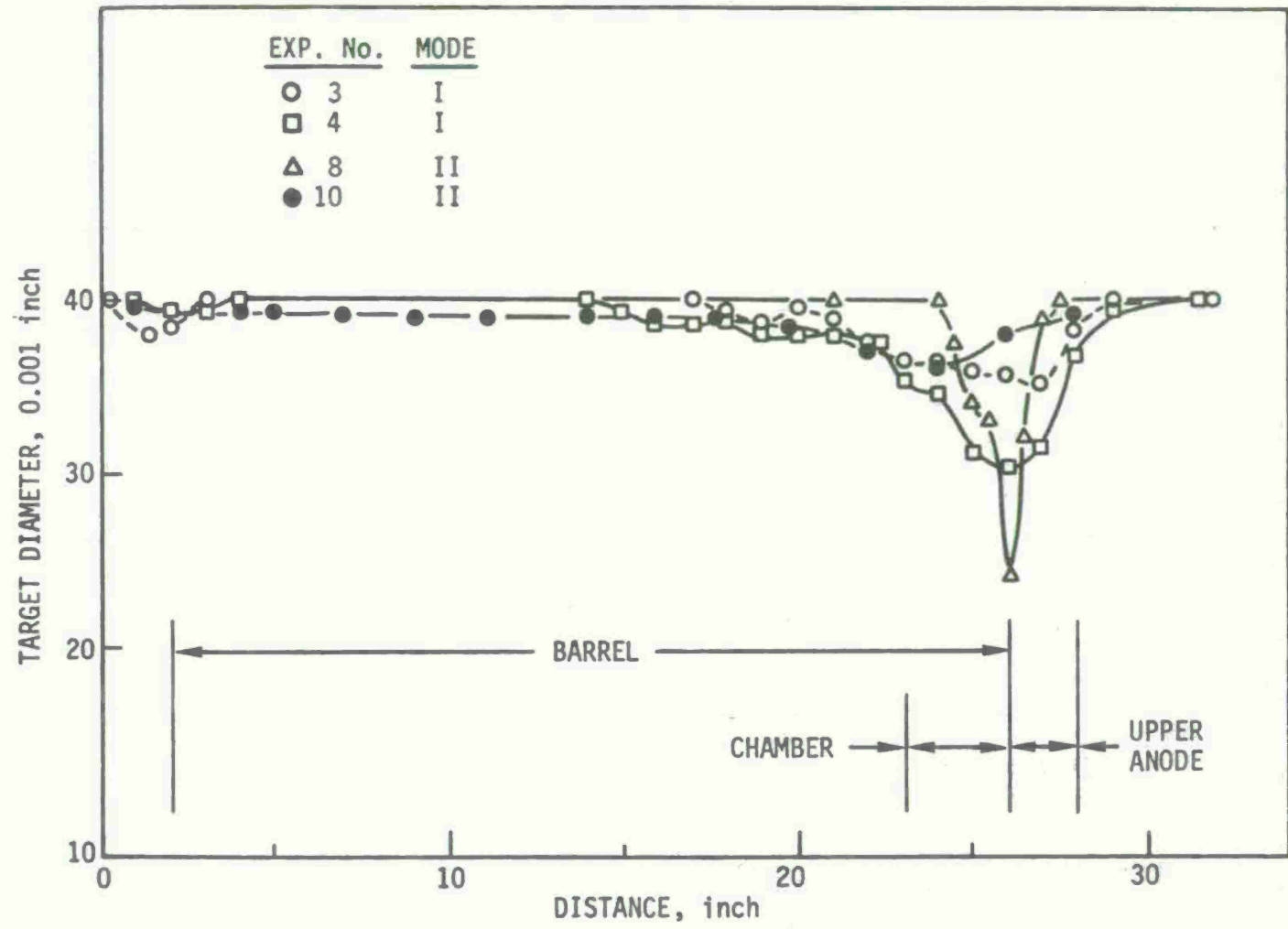


FIGURE 4. Measured target diameter vs. position within gun tube.

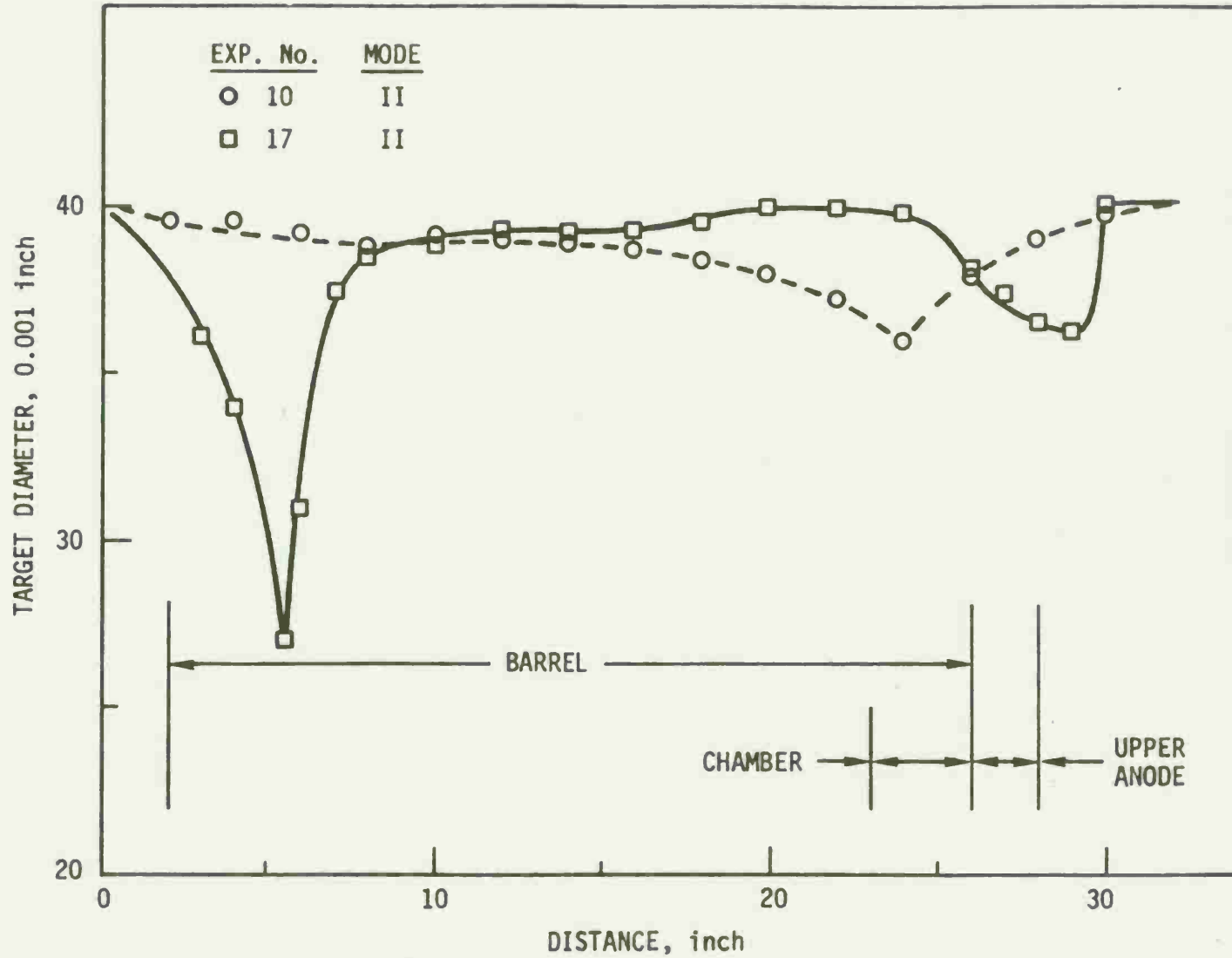
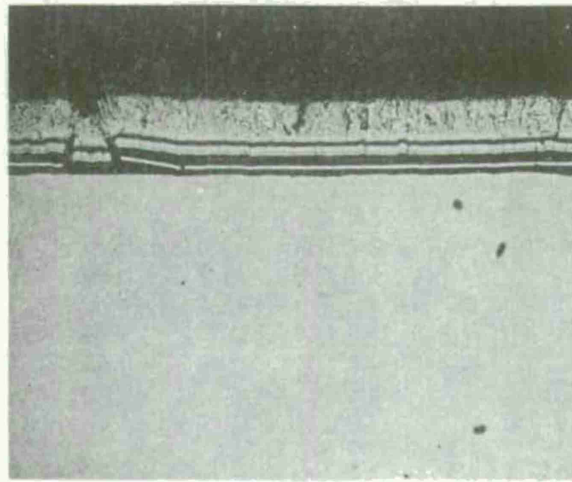
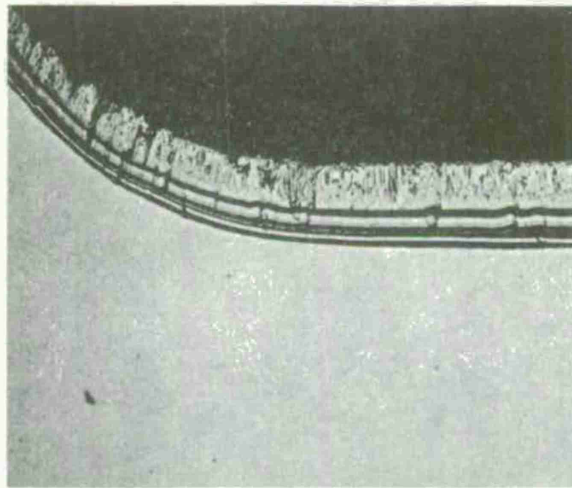


FIGURE 5. Measured target diameter vs. position within gun tube.



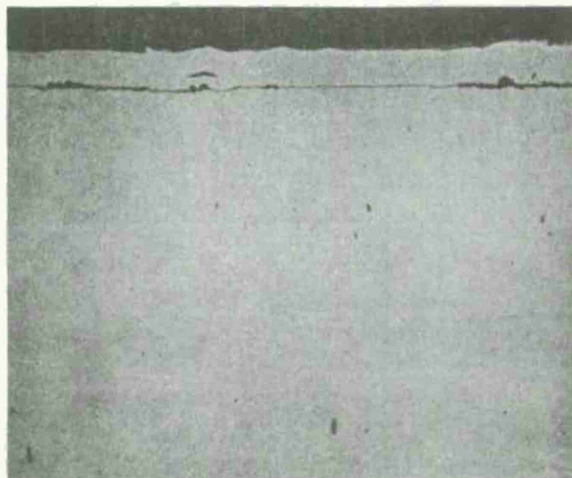
Muzzle end

(a)



Muzzle end, rifling

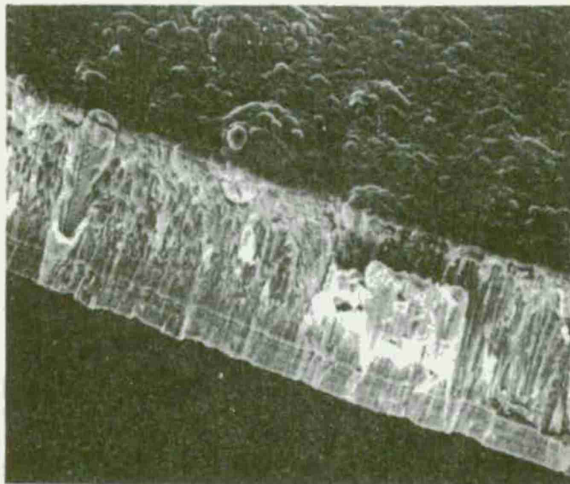
(b)



Chamber end

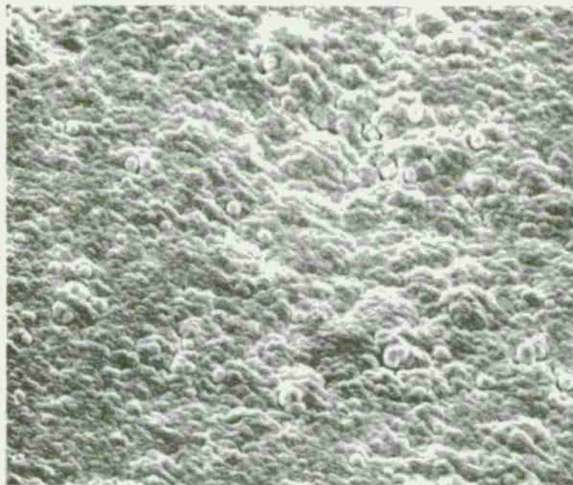
(c)

FIGURE 6. Optical photomicrographs of transverse section of 7.6 mm gun tube showing tungsten deposit. All 500X



Fracture surface.

(a)



Tungsten growth surface.

(b)

FIGURE 7. Scanning electron micrographs of tungsten deposit removed from muzzle end of 7.6 mm gun tube. 1500X

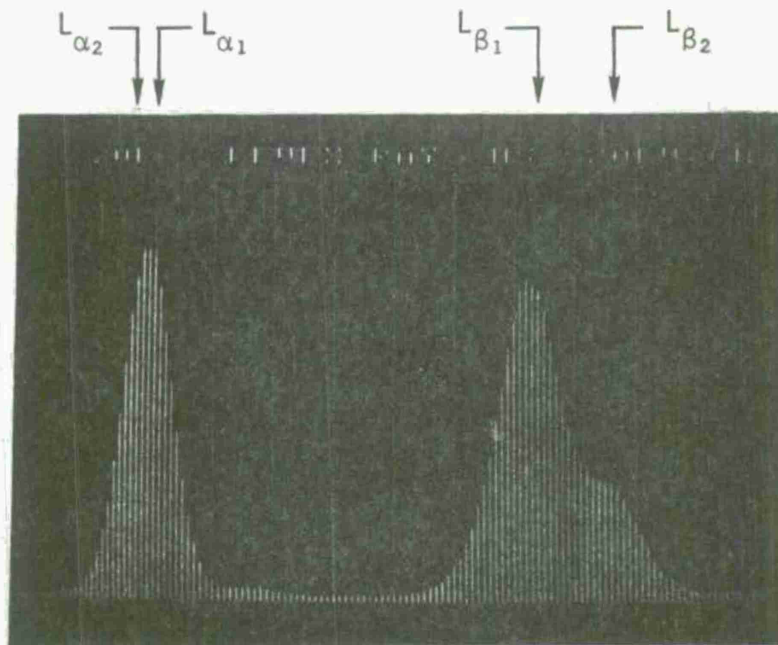


FIGURE 8. X-ray energy spectrograph of tungsten deposit with characteristic  $L_{\alpha}$  and  $L_{\beta}$  energies for tungsten indicated.

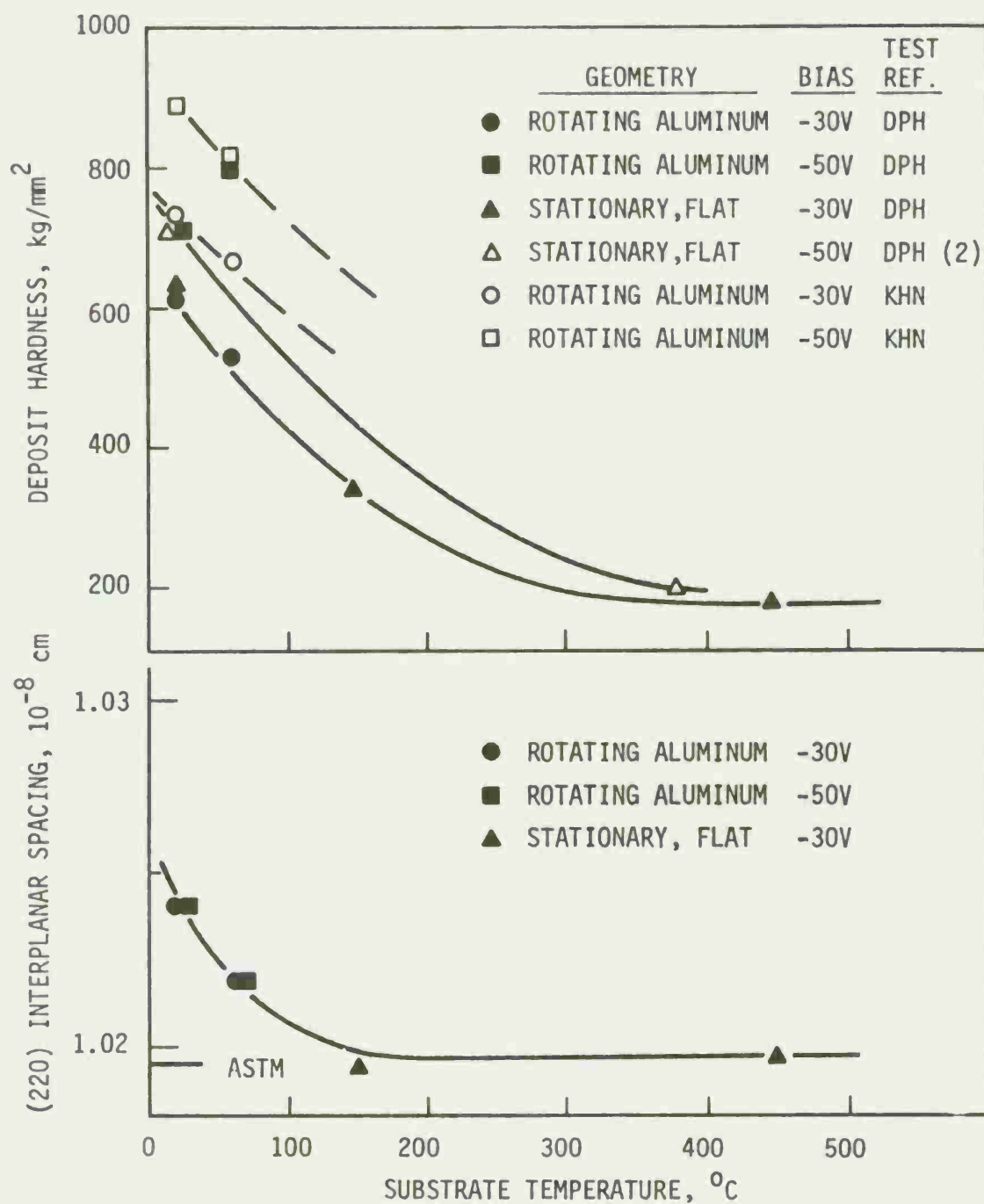
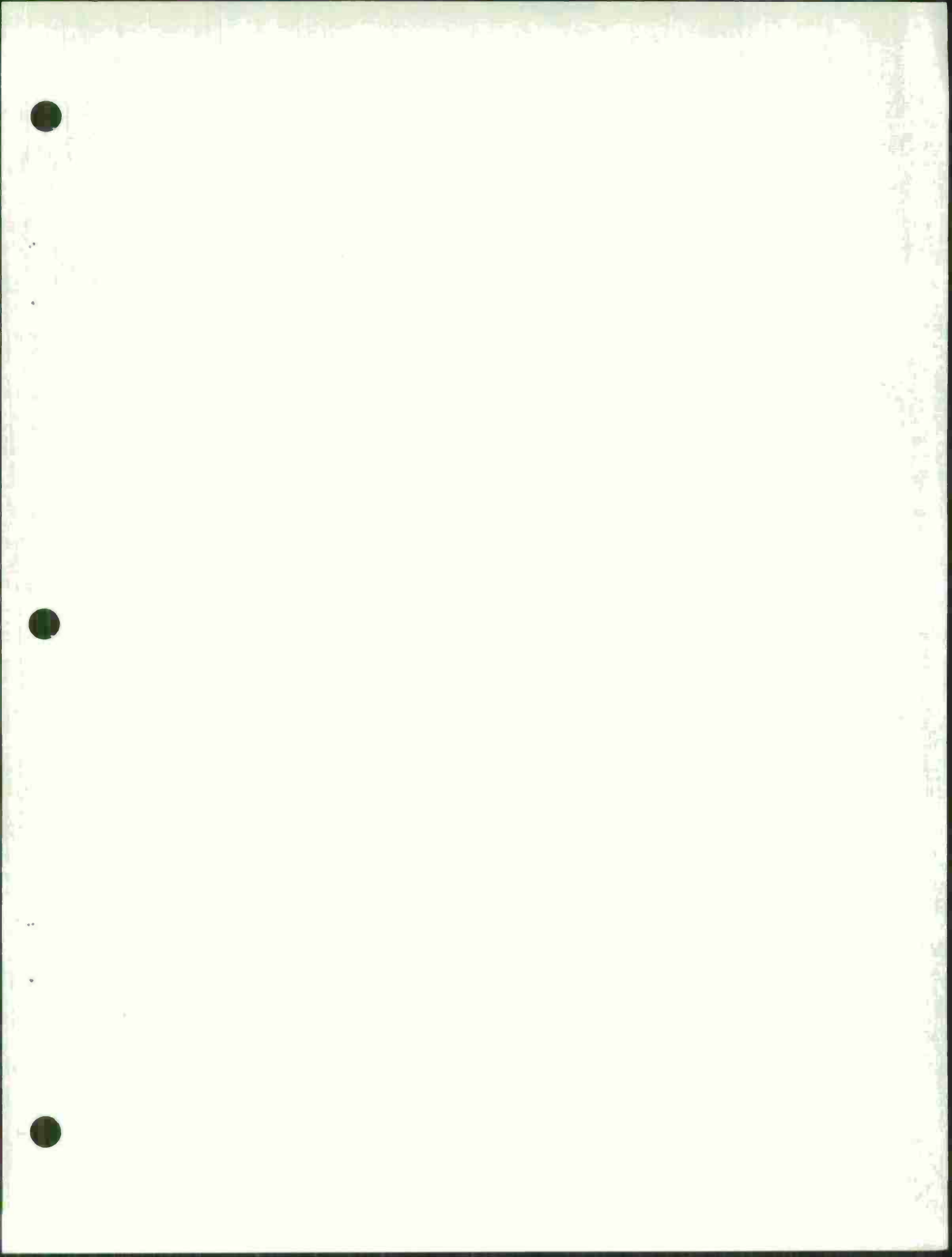
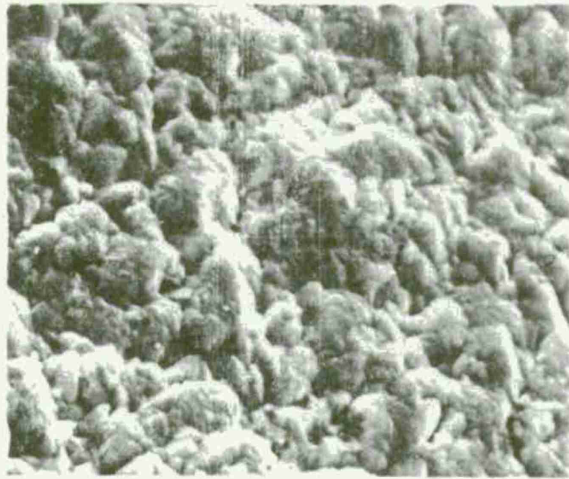


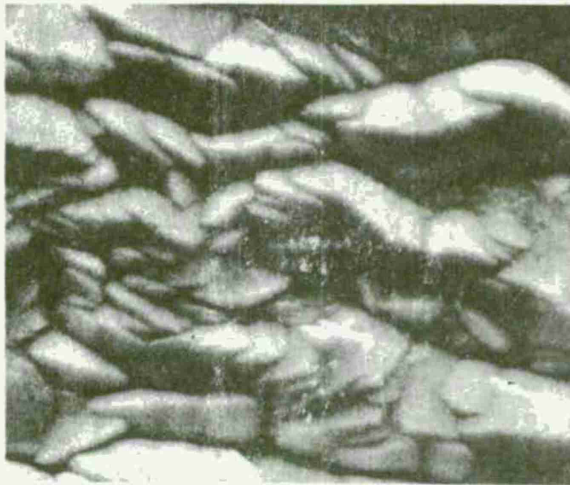
FIGURE 9. Deposit hardness and (220) interplanar spacing vs. substrate temperature for sputter-deposited chromium.





Deposit No. 2 .  
3000X

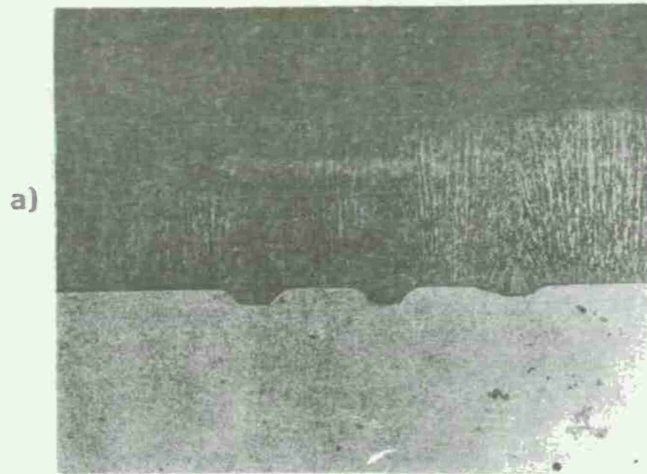
(a)



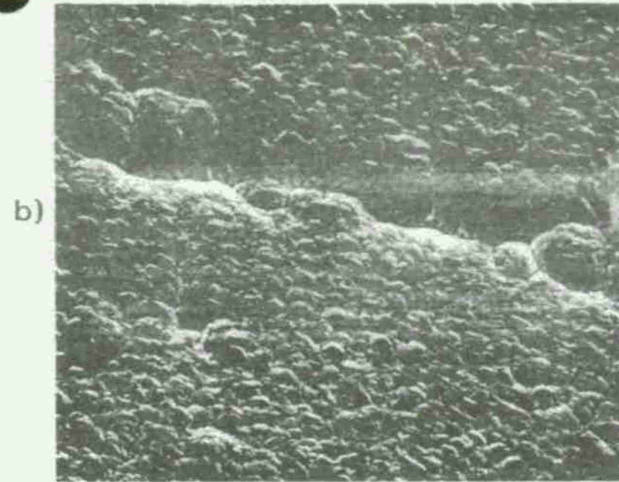
Deposit No. 4.  
4000X

(b)

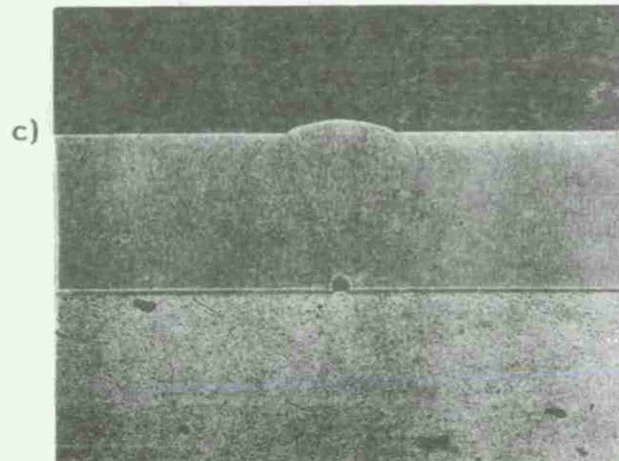
FIGURE 11. Sputter-deposited chromium growth surface.



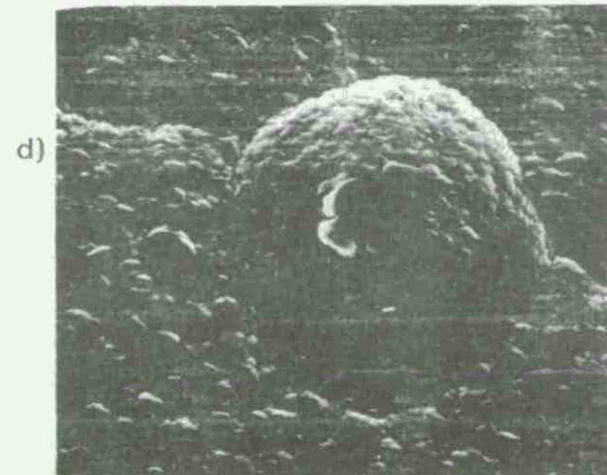
OM of deposit No. 2 showing longitudinal defects. 500X



SEM of deposit No. 2 . 600X

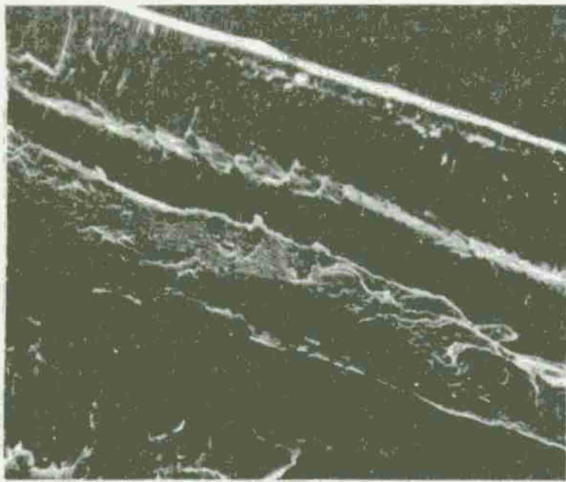


OM of deposit No. 1 showing defect nucleation at surface particle. 500X

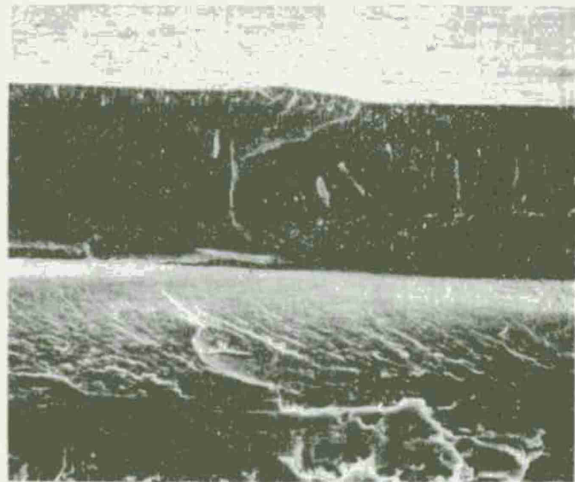


SEM of deposit No. 2 showing defect growth. 1200X

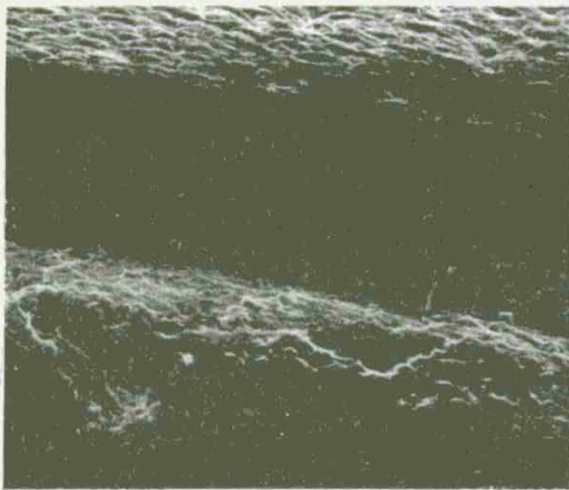
FIGURE 12. Optical (OM) and scanning electron (SEM) micrographs of sputter-deposited chromium showing some growth defects.



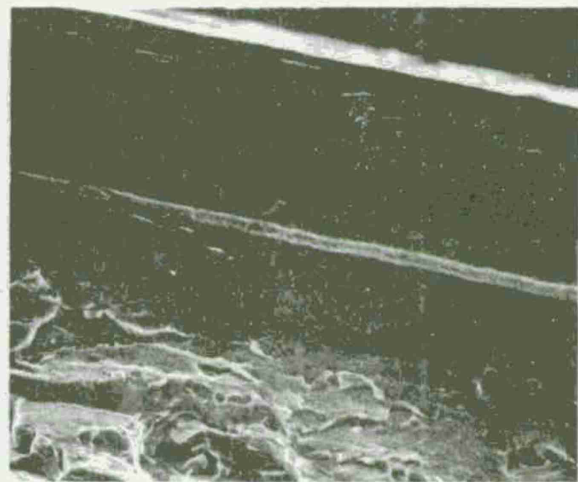
(a) Deposit No. 3. 800X



(b) Deposit No. 6. 600X



(c) Deposit No. 4. 800X



(d) Deposit No. 1. 400X

ALLOY  
ZONE

FIGURE 13. Sputter-deposited chromium fracture surfaces.

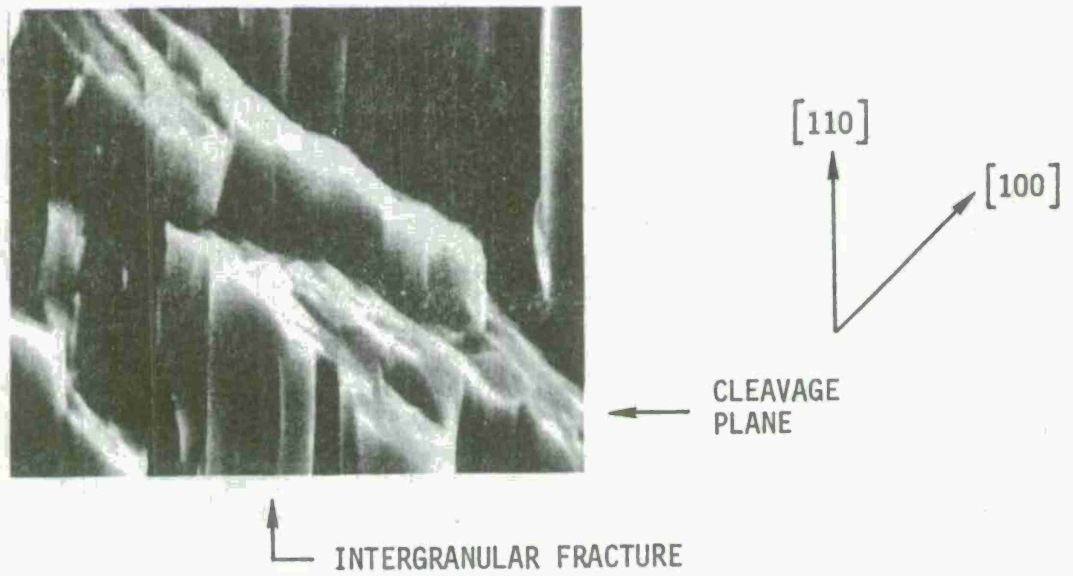


FIGURE 14. Scanning electron micrograph of deposit No. 2 fracture surface showing cleavage planes. 8000X

DISTRIBUTION

Copies

A. Department of Defense

Defense Documentation Center  
ATTN: TIPDR  
Cameron Station  
Alexandria, VA 22314

12

B. Department of the Army

Commander  
U. S. Army Materiel Development and Readiness Command  
ATTN: DCRD-E  
DRCRP-1  
DRCQA-E  
5001 Eisenhower Avenue  
Alexandria, VA 22333

1  
1  
1

Commander  
U. S. Army Materiel Development and Readiness Command  
Scientific and Technical Information Team - Europe  
ATTN: DRXST-STL Dr. Richard B. Griffin  
APO New York 09710

1

Commander  
U. S. Army Armament Command  
ATTN: DRSAR-PPI-K  
DRSAR-PPI-WW  
DRSAR-RDP  
DRSAR-SC  
DRSAR-QAE  
Rock Island, IL 61201

1  
1  
1  
1  
1

Director  
U. S. Army Materials and Mechanics Research Center  
ATTN: DRXMR-M  
Watertown, MA 02172

1

Director  
U. S. Army Maintenance Management Center  
ATTN: DRXMD-A  
Lexington, KY 40507

1

DISTRIBUTION

Copies

Commander  
U. S. Army Electronics Command  
ATTN: DRSEL-PP/1/IM  
Fort Monmouth, NJ 07703 1

Commander  
U. S. Army Missile Command  
ATTN: DRSMI-11E 1  
DRSMI-PRT 1  
Redstone Arsenal, AL 35809

Commander  
U. S. Army Tank-Automotive Command  
ATTN: DRSTA-RK 1  
DRSTA-RCM.1 1  
Warren, MI 48090

Commander  
U. S. Army Aviation Systems Command  
ATTN: DRSAV-ERE  
P. O. Box 209  
St. Louis, MO 63166 1

Commander  
U. S. Army Troop Support Command  
ATTN: DRSTS-PLC  
4300 Goodfellow Blvd.  
St. Louis, MO 63120 1

Commander  
Ballistic Missile Defense Systems  
ATTN: BNDSC-TS  
P. O. Box 1500  
Huntsville, AL 35804 1

Project Manager  
Munition Production Base Mod  
Picatinny Arsenal  
Dover, NJ 07801 1

Commander  
Harry Diamond Laboratories  
ATTN: DRXDO-RCD  
2800 Powder Mill Road  
Adelphi, MD 20783 1

DISTRIBUTION

Copies

Commander  
U. S. Army Natick Research and Development Command  
ATTN: DRXNL-EQ  
Kansas Street  
Natick, MA 01762

1

Commander  
U. S. Army Air Mobility R&D Labs  
ATTN: SAVDL-ST  
Fort Eustis, VA 23604

1

Commander  
Rock Island Arsenal  
ATTN: SARRI-PE  
SARRI-RS Mr. V. Long  
Rock Island, IL 61201

1

1

Commander  
Watervliet Arsenal  
ATTN: SARW-PPP-WP  
SARW-PPI-LAJ  
SARW-QA  
Watervliet, NY 12189

1

1

1

Commander  
Picatinny Arsenal  
ATTN: SARPA-MT-C  
SARPA-QA-T-T  
SARPA-C-C  
Dover, NJ 07801

1

1

1

Commander  
Frankford Arsenal  
ATTN: SARFA-T1000  
SARFA-QA  
SARFA-N5400  
Bridge & Tacony Streets  
Philadelphia, PA 19137

1

1

2

Commander  
Edgewood Arsenal  
ATTN: SAREA-QA  
Aberdeen Proving Ground, MD 21010

1

DISTRIBUTION

Copies

Director  
U. S. Army Production Equipment Agency  
ATTN: DRXPE-MT  
Rock Island Arsenal  
Rock Island, IL 61201 2

Director  
USDARCOM Intern Training Center  
ATTN: DRXMC-ITC-PPE  
Red River Army Depot  
Texarkana, TX 75501 1

Commander  
U. S. Army Tropic Test Center  
ATTN: STETC-MO-A (Technical Library)  
APO New York 09827 1

Commander  
Anniston Army Depot  
ATTN: DRXAN-DM  
Anniston, AL 36201 1

Commander  
Corpus Christi Army Depot  
ATTN: DRXAD-EFT  
Corpus Christi, TX 78419 1

Commander  
Fort Wingate Depot Activity  
ATTN: DRXFW-M  
Gallup, NM 87301 1

Commander  
Letterkenny Army Depot  
ATTN: DRXLE-M 1  
DRXLE-MM 1  
Chambersburg, PA 17201

Commander  
Lexington-Blue Grass Army Depot  
ATTN: DRXLX-SE-1  
Lexington, KY 40507 1

DISTRIBUTION

Copies

Commander  
New Cumberland Army Depot  
ATTN: DRXNC-SM  
New Cumberland, PA 17070

1

Commander  
Pueblo Army Depot  
ATTN: DRXPU-ME  
          DRXPU-SE  
Pueblo, CO 81001

1

1

Commander  
Red River Army Depot  
ATTN: DRXRR-MM  
Texarkana, TX 75501

1

Commander  
Sacramento Army Depot  
ATTN: DRXSA-MME-LB  
Sacramento, CA 95813

1

Commander  
Seneca Army Depot  
ATTN: DRXSE-SE  
Romulus, NY 14541

1

Commander  
Sharpe Army Depot  
ATTN: DRXSH-SO  
          DRXSH-M  
Lathrop, CA 95330

1

1

Commander  
Sierra Army Depot  
ATTN: DRXSI-DQ  
Herlong, CA 96113

1

Commander  
Tobyhanna Army Depot  
ATTN: DRXTO-ME-B  
Tobyhanna, PA 18466

1

DISTRIBUTION

	<u>Copies</u>
Commander Tooele Army Depot ATTN: DRXTE-SEN DRXTE-EMD Tooele, UT 84074	1 1
Commander Badger Army Ammunition Plant Baraboo, WI 53913	1
Commander Holston Army Ammunition Plant Kingsport, TN 37660	1
Commander Indiana Army Ammunition Plant Charleston, IN 47111	1
Commander Iowa Army Ammunition Plant Burlington, IA 52602	1
Commander Joliet Army Ammunition Plant Joliet, IL 60434	1
Commander Lone Star Army Ammunition Plant Texarkana, TX 75501	1
Commander Louisiana Army Ammunition Plant P. O. Box 30058 Shreveport, LA 71161	1
Commander Milan Army Ammunition Plant Milan, TN 38358	1
Commander Newport Army Ammunition Plant Newport, IN 47966	1

DISTRIBUTION

Copies

Commander  
Radford Army Ammunition Plant  
Radford, VI 24141 1

Commander  
Ravenna Army Ammunition Plant  
Ravenna, OH 44266 1

Commander  
Riverbank Army Ammunition Plant  
Riverbank, CA 95367 1

Commander  
Scranton Army Ammunition Plant  
Scranton, PA 18501 1

Commander  
Sunflower Army Ammunition Plant  
Lawrence, KS 66044 1

Commander  
Twin Cities Army Ammunition Plant  
New Brighton, MN 55112 1

Commander  
Volunteer Army Ammunition Plant  
ATTN: SARVO-T  
P. O. Box 6008  
Chattanooga, TN 37401 1

C. Department of the Navy

Officer in Charge  
U. S. Navy Materiel Industrial Resources Office  
ATTN: Code 227  
Philadelphia, PA 19112 1

D. Department of the Air Force

Commander  
Air Force Materials Laboratory  
ATTN: LTE 1  
LTM 1  
LTN 1  
Dayton, OH 45433

DISTRIBUTION LIST UPDATE

- - - FOR YOUR CONVENIENCE - - -

Government regulations require the maintenance of up-to-date distribution lists for technical reports. This form is provided for your convenience to indicate necessary changes or corrections.

If a change in our mailing lists should be made, please check the appropriate boxes below. For changes or corrections, show old address *exactly* as it appeared on the mailing label. Fold on dotted lines, tape or staple the lower edge together, and mail.

Remove Name From List

Change or Correct Address

Old Address:

Corrected or New Address:

COMMENTS

---

---

---

---

---

Date: \_\_\_\_\_ Signature: \_\_\_\_\_

Technical Report #

FOLD HERE

Return Address:

POSTAGE AND FEES PAID  
DEPARTMENT OF THE ARMY  
DOD 314



OFFICIAL BUSINESS  
*Penalty for Private Use \$300*

Commander  
Rock Island Arsenal  
Attn: SARRI-LR  
Rock Island, Illinois 61201

FOLD HERE

AD  
CDR, Rock Island Arsenal  
GEN Thomas J. Rodman Lab  
Rock Island, IL 61201

Accession No. \_\_\_\_\_  
Pacific Northwest Laboratories  
a division of  
Battelle Memorial Institute  
P.O. Box 999  
Richland, Washington 99352

UNCLASSIFIED

1. Sputter deposition
2. Coating on Gun Tubes
3. Tungsten Coating
4. Chromium Coating

THE SPUTTER DEPOSITION AND EVALUATION OF TUNGSTEN AND CHROMIUM FOR USE IN WEAPON COMPONENTS, by R.H. Jones, R.W. Moss, E.D. McClanahan and H.L. Butts - Pacific Northwest Laboratories.

Report R-TR-75042, Oct 75, 41 p. Incl. illus. tables, (Contract MIPR M5-4-P0048-01-M5-W3, AMS Code 3297.06. 7501) Unclassified report.

This work was conducted to establish sputter deposition as a candidate production coating process for military items. Specifically two areas were evaluated -- deposition on internal bore surfaces of gun barrels and deposition of wear resistant coatings on external surfaces.

DISTRIBUTION  
Copies obtainable  
from DDC

AD  
CDR, Rock Island Arsenal  
GEN Thomas J. Rodman Lab  
Rock Island, IL 61201

Accession No. \_\_\_\_\_  
Pacific Northwest Laboratories  
a division of  
Battelle Memorial Institute  
P.O. Box 999  
Richland, Washington 99352

UNCLASSIFIED

1. Sputter deposition
2. Coating on Gun Tubes
3. Tungsten Coating
4. Chromium Coating

THE SPUTTER DEPOSITION AND EVALUATION OF TUNGSTEN AND CHROMIUM FOR USE IN WEAPON COMPONENTS, by R.H. Jones, R.W. Moss, E.D. McClanahan and H.L. Butts - Pacific Northwest Laboratories.

Report R-TR-75042, Oct 75, 41 p. Incl. illus. tables, (Contract MIPR M5-4-P0048-01-M5-W3, AMS Code 3297.06. 7501) Unclassified report.

This work was conducted to establish sputter deposition as a candidate production coating process for military items. Specifically two areas were evaluated -- deposition on internal bore surfaces of gun barrels and deposition of wear resistant coatings on external surfaces.

DISTRIBUTION  
Copies obtainable  
from DDC

The feasibility of sputter deposition on bore surfaces of 7.62mm gun tubes was studied using both a modified dc-triode scheme with tungsten targets centered on the gun tube axis and a dc-diode scheme with the plasma supported by thermally emitted electrons from a hot target/filament centered on the gun tube axis. Although the latter scheme gave better deposition characteristics, further refinements appear necessary before the method can be adapted as a production coating process. High quality chromium coatings were produced on 7076-T6 aluminum substrates in the work involving deposition on external surfaces. The wear test results indicate the sputter deposited chromium coatings exhibited superior substrate adherence and more uniform wear characteristics when compared to the electro-deposited chromium plating.

The feasibility of sputter deposition on bore surfaces of 7.62mm gun tubes was studied using both a modified dc-triode scheme with tungsten targets centered on the gun tube axis and a dc-diode scheme with the plasma supported by thermally emitted electrons from a hot target/filament centered on the gun tube axis. Although the latter scheme gave better deposition characteristics, further refinements appear necessary before the method can be adapted as a production coating process. High quality chromium coatings were produced on 7076-T6 aluminum substrates in the work involving deposition on external surfaces. The wear test results indicate the sputter deposited chromium coatings exhibited superior substrate adherence and more uniform wear characteristics when compared to the electro-deposited chromium plating.



